Feasibility of silica hybridized collagen hydrogels as three-dimensional cell matrices for hard tissue engineering

Hye-Sun Yu[a,b], Eun-Jung Lee[a,b], Seog-Jin Seo[a,b], Jonathan C. Knowles[b,c], Hae-Won Kim[a,b,d,*]

[a] Institute of Tissue Regeneration Engineering (ITREN), Dankook University, Cheonan 330-714, Republic of Korea

[b] Department of Nanobiomedical Science and BK21 PLUS NBM Global Research Center for Regenerative Medicine, Dankook University Graduate School, Cheonan 330-714, Republic of Korea

[c] Division of Biomaterials and Tissue Engineering, Eastman Dental Institute, University College London, 256 Gray's Inn Road, London WC1X 8LD, UK

[d] Department of Biomaterials Science, College of Dentistry, Dankook University, Cheonan 330-714, Republic of Korea

---

*Corresponding author: Prof. H.-W. Kim (e-mail: kimhw@dku.edu; tel: +82 41 550 3081; fax: +82 41 550 3085)

***For*: Journal of Biomaterials Applications**

Abstract

Exploiting hydrogels for the cultivation of stem cells, aiming to provide them with physico-chemical cues suitable for osteogenesis, is a critical demand for bone engineering. Here, we developed hybrid compositions of collagen and silica into hydrogels via a simple sol-gel process. The physico-chemical and mechanical properties, degradation behavior, and bone-bioactivity were characterized in-depth; furthermore, the in vitro mesenchymal stem cell growth and osteogenic differentiation behaviors within the 3D hybrid gel matrices were communicated for the first time. The hydrolyzed and condensed silica phase enabled chemical links with the collagen fibrils to form networked hybrid gels. The hybrid gels showed improved chemical stability and greater resistance to enzymatic degradation. The in vitro apatite-forming ability was enhanced by the hybrid composition. The viscoelastic mechanical properties of the hybrid gels were significantly improved in terms of the deformation resistance to an applied load and the higher modulus values under a dynamic oscillation. Mesenchymal stem cells adhered well to the hybrid networks and proliferated actively with substantial cytoskeletal extensions within the gel matrices. Of note, the hybrid gels substantially reduced the cell-mediated gel contraction behaviors, possibly due to the stiffer networks and higher resistance to cellular degradation. Furthermore, the osteogenic differentiation of MSCs, including the expression of bone-associated genes and protein, was significantly upregulated within the hybrid gel matrices. Together with the physico-chemical and mechanical properties, those MSCs behaviors observed within 3D gel matrices, being different from the previous approaches reported on 2D substrates, provide new information on the feasibility and usefulness of the silica-collagen system as the 3D bio-matrices for stem cell culture and tissue engineering of hard tissues.

Keywords: Bone tissue engineering; Collagen gel; Hybrids; Osteogenesis; Silica; Stability;

1. Introduction

Hydrogels have gained considerable attention as a matrix within which to culture tissue cells since they provide 3-dimensional (3D) scaffold environment for cells to properly adhere, spread and grow, and to acquire tissue-specific differentiation cues.[1-4] The high water content and tissue-like elastic properties of hydrogels make them ideal candidates as 3D matrices for cell encapsulation and delivery for engineered tissues.[5-8] Furthermore, bioactive signaling molecules can be integrated within hydrogel networks to improve therapeutic functions in regulation of cellular fate.[9, 10] For hydrogels to provide 3D matrix conditions favorable to cells for target tissue development, the physico-chemical and mechanical properties, as well as the degradation profile should be carefully tailored.

Among other materials, polymers of natural origin, such as collagen, alginate, and chitosan as hydrogels, have been widely used and developed due to their excellent cellular affinity and tissue compatibility.[2, 11] In particular, collagen, as the most abundant protein present in mammals, has been the most frequent option for culture of cells and repair and regeneration of diverse tissues including bone and teeth.[10, 12] However, there some critical limitations that have been encountered, particularly for use in hard tissues, such as poor mechanical properties and rapid degradation.[13, 14] Furthermore, in cell cultures, collagen is known to undergo substantial shrinkage, limiting its potential for applications in wound repair and defect closure.[15] With their relatively low chemical stability and low physical rigidity, collagen hydrogels have primarily been used to target soft tissues rather than for hard tissues.

Physical compression of collagen has been conducted to overcome these limitations and to improve the properties of collagen-based hydrogels. The compressed collagen showed a condensed structure, resulting in higher physical and mechanical properties that are more favorable for hard tissue applications.[16]

The combination of collagen with inorganic nanomaterials, has also gained great attention to improve the properties of collagen-based biomaterials. Some nanocomposites or hybridized collagen-based hydrogels, such as collagen/apatite and collagen/bioactive glass, have been recognized to exhibit improved mechanical and biological properties that are more suitable for bone repair.[16-18] However, studies on hydrogels with nanocomposite/hybrid compositions have not been investigated as rigorously. One recent elegant study on collagen hydrogels that incorporated surface-

functionalized bioactive glass nanoparticles showed an improved physico-chemical stability and the associated gel properties against shrinkage during cell culture.[16]

Here, we aimed to produce hybrid hydrogels based on collagen and silica. The composition was amenable to in situ gelation, culture of cells, and hard tissue engineering. In fact, the collagen/silica hybrid compositions have been documented in the form of coatings, membranes, and gels, and the preparation methods and the properties related to the cells have been reported. The sol-gel process introduced has been shown to be effective in generating collagen-silica hybrid networks.[19, 20] The hardened hybrid materials, with a mesoporous structure, have presented controlled drug release, suggesting that they are suitable as drug delivery matrices.[21] The dried collagen/silica membranes have also been shown to improve in vitro and in vivo bioactivity for use as guiding membranes for bone regeneration.[22-27] While the collagen/silica hybrid compositions have been shown to hold potential properties for use in bone repair and regeneration, very few systematic works have been carried out on hybrid hydrogels to encapsulate and cultivate cells for cell delivery and bone tissue engineering.

In the present study, collagen/silica hybrid hydrogels were prepared through a simple sol-gel process during which cells were simultaneously cultivated to provide hybrid gel 3D networks. The physico-chemical and mechanical properties, as well as the degradation of the hybrid hydrogels were investigated, and the cell-associated gel contraction was also monitored. Furthermore, the cell growth and osteogenic differentiation behaviors were compared. Such a series of properties evaluated were judged to determine the efficacy of the hybrid compositions as 3D hydrogel matrices for hard tissue engineering. While many studies on silica-collagen system have explained cellular phenomena over the 2D substrates, this study is considered to report for the first time on the cell behaviors within silica-collagen 3D gel matrix conditions.

2. Experimental Part

2.1. Preparation of silica-collagen solutions and hydrogels

Tetramethyl orthosilane (TMOS) was chosen as a silica source and was hydrolyzed for 3 h at room temperature by adding water under acidic conditions (1 N HCl). The molar ratio of TMOS to water was 1:10 in order to minimize redundant liquid. A collagen solution (3.87 mg/ml, rat tail Col I; BD

Biosciences) was diluted in distilled water at a concentration of 3.5 mg/ml. The collagen solution was mixed with hydrolyzed TMOS at weight ratios of collagen:TMOS = 90:10 and 80:20, called Col-10S and Col-20S, respectively. The mixtures were then placed in spinner flasks and were stirred with a magnetic stirrer at 50 rpm in an ice bath. Dulbecco's-modified eagle medium (10X)-based cell suspensions were added to the solution, which was then neutralized with 0.5 N NaOH.[28] The mixtures were cast in a plastic mould (6 mm x 3 mm) and were shortly incubated at 37 °C for 1 h for gelation.

2.2. Sample characterization

The surface morphology was observed via scanning electron microscopy (SEM; Hitachi). Hydrogel samples were washed with distilled water several times, and then freeze-dried for the SEM. The atomic composition was detected using energy dispersive spectroscopy (EDS; Bruker) attached to SEM. The chemical composition was examined via attenuated total reflectance-Fourier transform infrared (ATR-FTIR; Varian 640-IR) analysis. The transmission spectra were recorded in the spectral range of 4000–400 cm^{-1} with a resolution of 4 cm^{-1}. The release of silicon ion from the samples was investigated by incubation of the freeze-dried sample in 10 ml of phosphate buffered saline (PBS at pH 7.4) solution at 37 ^{o}C. At each period, the release of Si ion was detected using Si titration with inductively coupled plasma atomic emission spectrometry (ICP-AES). The thermal stability was assessed with differential scanning calorimetry (DSC, Q-20, TA Instruments), and the measurements were conducted in the temperature range from 20 to 100 °C with 5 °C/min heating rate under a nitrogen flow.

2.3. Enzymatic degradation tests

For the enzymatic degradation test, collagenase type I (Worthington Biochemical, USA) was used. Each sample with a cylindrical shape (6 mm x 3 mm) was incubated in 1 ml of 0.1 M Tris–HCl buffer (pH 7.4) containing 50 mM $CaCl_2$ at 37 °C. Collagenase type I was prepared at a specific concentration (54 units/ml in 0.1 M Tris–HCl). The samples were soaked within a collagenase solution for 30, 60, and 120 min, which was then placed on ice at 4 °C and was added 0.2 ml of 0.25 M EDTA. The weight change in the samples during the test was recorded. Three replicate samples were used for the test.

2.4. In vitro apatite mineralization test

The *in vitro* apatite forming ability of the samples was tested in Kokubo's simulated body fluid (SBF, pH 7.4) at 37 °C.[29] SBF was prepared by dissolving NaCl (142.0 mM), $NaHCO_3$ (4.2 mM), KCl (5.0 mM), $K_2HPO_4.3H_2O$ (1.0 mM), $MgCl_2.6H_2O$ (1.5 mM), $CaCl_2$ (2.5 mM), and Na_2SO_4 (0.5 mM) into deionized water buffered to pH 7.4 with Tris-HCl buffer at 37 °C. The lyophilized hydrogels were cut into proper sizes and were subsequently placed in 6-well plates containing 10 ml SBF in each well, which were then incubated at 37 ºC for up to 7 days with a refreshed SBF solution every day. Three replicate samples were used for the SBF test After removal from the SBF, the samples were washed with distilled water, and were then dried at room temperature. The formation of apatite crystals was examined via X-ray diffraction (XRD, Ultima IV, Rigaku, Japan) and SEM. The nano-crystalline morphology was examined by using high resolution transmission electron microscopy (HR-TEM), and the crystal pattern was analyzed according to the selected area electron diffraction (SAED). For the TEM observation, the samples were washed several times with distilled water, freeze-dried, and then a part of the samples was scratched off to place on a Cu grit.

2.5. Static and dynamic mechanical tests

The viscoelastic measurements were performed using a dynamic mechanical analyzer (DMA 25N, 01dB-Metravib, France) where samples in hydrated state with cylindrical geometry and dimensions of 10 x 10 x 15 mm^3 were used. Two types of compression stress tests, including static and dynamic tests, were performed on the prepared hydrogels. The static compression stress test, a sort of creep test, involves the application of a constant static compressive stress of 0.5 kPa normal to the cylindrical hydrogel sample axis, and the strain of the sample was measured as a function of time at room temperature for 450 s. For the dynamic compression stress test, the upper cylindrical rod was allowed to oscillate sinusoidally with small strain amplitude (100 μm) which was in the linear range of viscoelasticity of the material. The tests were conducted using a frequency ranging from 0.5 up to 10 Hz for 10 min at room temperature. The storage (E') and loss (E'') modulus of the samples were measured, and the energy loss (tan delta; E''/E') value was also calculated.

2.6. Mesenchymal stem cells (MSCs) and culture in hydrogels

MSCs derived from rat bone marrow were isolated from adult Sprague-Dawley rats (5 weeks old). The proximal and distal epiphyses of the rat femora and tibiae were cut off, and bone marrow tissue was flushed out with a collagenase type I solution in alpha-minimal essential medium (MEM). The tissue was centrifuged and re-suspended in a normal culture medium (alpha-MEM supplemented with 10% fetal bovine serum containing 1% penicillin/streptomycin) and was then placed in a culture dish in an incubator under a humidified atmosphere of 5% CO_2 in air at 37 °C. The adherent cells were expanded and sub-cultured for 3 passages for further experiments.

For the culture of MSCs within the hydrogels, the cells were prepared at a concentration of 1 x 10^5 cells/ml in the 1 ml of the hydrogel solution, which was allowed to gel during storage at 37 ^oC for 1 h. The cell-hydrogel constructs were cultured in an osteogenic medium (normal medium plus 50 μg/ml sodium ascorbate, 10^{-2} M sodium β-glycerol phosphate and 10^{-8} M dexamethasone) for up to 3 weeks. The cell-gel constructs were prepared in each well of 24-well plates for further analyses, including cell growth, morphology, and osteogenic differentiation. For the biological assays, the cells were harvested by digesting the hydrogels with collagenase type I (10 mg/ml) and then separating them via a centrifugation (1500 rpm).

2.7. Hydrogel contraction test

The hydrogel contraction due to the cells present inside was also recorded. Different concentrations of cells (5 x 10^4, 1 x 10^5, and 2 x 10^5 cells/ml) were used for the test. Cell-hydrogel constructs were prepared in each well of 6-well plates, and the diameter change of the hydrogels was recorded during the culture. Samples were tested in triplicate.

2.8. Cell viability and growth morphology

Cell viability was assessed using an MTS [3-(4, 5-dimethylthiazol-2-yl)-5-(3-carboxymethoxyphenyl)-2-(4-sulfophenyl)-2H tetrazolium] assay kit (CellTiter 96 Aqueous One Solution from Promega) using a spectrophotometer at an absorbance of 490 nm.

The growth morphology of cells in the hydrogels was observed via confocal laser scanning microscopy (CLSM; LSM 510, Carl Zeiss). The cells were fixed with 4% paraformaldehyde and were permeabilized in 0.1% Trion X-100 for 5 min. An Alexa Fluor 546 phalloidin (Invitrogen A22283)

198 solution diluted in PBS was added into the sample. ProLongVR Gold antifade reagent with 40,6-
199 diamidino-2-phenylindole (DAPI) (Invitrogen P36935) was used to stain nuclei.

200

201 ***2.9. Gene expression by quantitative polymerase chain reaction (QPCR)***

202 The expression of genes associated with osteogenesis, including Runx-2, osteopontin (OPN), and
203 bone sialoprotein (BSP), was assessed via QPCR. The total RNA was extracted from the lysate of
204 cells gathered from each scaffold using the RNeasy Kit (Qiagen). The isolated RNA was quantified
205 using Quant-It RiboGreen kit. Total RNA (50 ng) was reverse-transcribed to cDNA with a first-strand
206 cDNA synthesis kit (PrimeScript RT reagent Kit, Bioneer) using random hexamers as primers. Finally,
207 QPCR was performed using Sensimix Plus SYBR master mix (Quantace) in a spectrofluorometric
208 thermal cycler (Rotor-Gene 3000; Corbett Research). Comparative threshold cycle (CT) method was
209 used where the accumulated PCR products for each gene examined were normalized in accordance
210 with the reference gene, GAPDH, and triplicate samples were tested. The primer sequences of the
211 genes for QPCR are as follows: GAPDH: GATGACATCAAGAAGGTGGT (forward), CAAAGTTGTCA
212 TTGAGAGCA (reverse); OPN: CCGATGAATCTGATGAGTCCTT (forward), TCCAGCT
213 GACTTGACTCATGG (reverse); BSP: ATCAAAGCAGAGGATTCTGA (forward), TTCG
214 TTGTTTTCCTCTTCAT (reverse).

215

216 ***2.10. Protein expression by Western blot***

217 Based on the results of the QPCR, the expression of protein BSP was analyzed via Western blotting.
218 The extracts of the cells harvested after 14 days of culture were prepared with a RIPA buffer, after
219 which the protein samples were resolved on 10% SDS-polyacrylamide gels, transblotted to NC
220 membranes blocked with 2.5% BSA in Tris-buffered saline with 0.1% Tween-20, and were probed
221 with primary antibody (anti-BSP antibody, 1:1000). The blots were then incubated with HRP-
222 conjugated secondary IgG, and immunoreactive bands were detected using an ECL detection reagent
223 (Pierce, Rockford).

224

2.11. Statistical analysis

Data were represented as means and standard deviations. The data comparison was carried out using a Student's t-test, and the significance level was considered at $p < 0.05$.

3. Results and Discussion

3.1. Physico-chemical and degradation properties of the hybrid hydrogels

The schematic view of the collagen/silica (Col/Sil) hybrid networks formed in the hydrogels is depicted in **Fig. 1**. The silica precursor silane molecules hydrolyzed and then polymerized to form siloxane (Si-O-Si) networks. On the other hand, collagen molecules self-assembled into a fibrillar formation. In the meantime, the siloxane end groups and the functional groups present in the amino acid sequences of the collagen fibrils chemically interacted to be hybridized and gelled.[19, 30]

The chemical interactions of the hydrogels were further characterized via FT-IR (**Fig. 2a**). Pure Col showed typical amide bands. The Col/Sil hybrids showed a development of bands in very similar positions to those of Col. However, on closer examination, the amide bands of Col/Sil showed a slight blue shift (dashed lines in **Fig. 2b**). The results indicated that there were possible chemical interactions between the collagen and silica, i.e., the amino acids of collagen with the siloxane group of the silica composition. Based on DSC curves of the different gel compositions a difference in the denaturation temperature of the collagen was determined: ~36.5 °C for pure Col, which increased to ~50 °C for both hybrids (**Fig. 2c**). This was also possibly due to the effects of the silica-collagen chemical interactions. In previous reports on collagen nanocomposites with inorganic hydroxyapatite nanocrystals, such an improvement in the denaturation point of collagen has also been reported.[31, 32]

After confirming that there was a strong chemical interaction between the collagen and silica in the hydrogels, we next examined the degradation behavior. The enzymatic degradation of the hydrogels was also analyzed by exposure to collagenase type I. During soaking each hydrogel in collagenase I for up to 120 min, the weight loss of the samples was monitored (**Fig. 3**). With increasing silica content, the weight loss decreased; 100% for collagen, 89% for Col-10S, and 65% for Col-20S at 120 min after soaking. Considering the silica content in each hydrogel, i.e., 0%, 10% and 20% for collagen, Col-10S, and Col-20S, respectively, the silica-added hybrid hydrogels showed

a lower degradation level. The results indicated that the increase in silica improved the resistance to the enzymatic degradation of collagen. Taken together, the hybrid composition improved the enzymatic degradation of hydrogels.

3.2. Mechanical properties of the hybrid hydrogels under static and dynamic conditions

Along with the degradation behavior, the mechanical properties of the hydrogels were analyzed. First, the hydrogels experienced a static load, and the strain change was recorded against time for up to 450 s (**Fig. 4a**). With time, the static strain of the collagen increased rapidly followed by a continual decreased stain rate, while the Col/Sil hydrogels showed substantially decreased strain change, especially, with increasing silica content. The initial strain rate was measured to be ~2 x 10^{-5}/s, ~4 x 10^{-6}/s, and ~4 x 10^{-7}/s, for collagen, Col-10S, and Col-20S, respectively. Furthermore, the static strain recorded at 450 s was ~0.037, 0.019 and 0.007 on average, for collagen, Col-10S, and Col-20S, respectively (**Fig. 4b**). The static mechanical tests demonstrated that the silica-added hybrid gels sustained a static load and thus resisted the deformation more effectively.

Next the dynamic mechanical properties of the hydrogels were investigated via DMA. The hydrogel samples were subjected to a dynamic load with a varying frequency of over 0.5–10 Hz, and the storage modulus (E') and the loss modulus (E") values were recorded. E' values of all the samples changed very little with frequency. Interestingly, the E' value of Col-20S showed the most striking increase compared to that of other samples (**Fig. 5a**). The E" values increased with frequency, and higher E" values were recorded with an increase in silica content. The E' and E" values were averaged and showed significant increases with an increase in silica content, and E" value in Col-20S was the highest and showed the most increase (**Fig. 5b**). The energy loss factor E"/E' (tan delta) showed a slight decrease with an increase in silica (**Fig. 5c**). The DMA results demonstrated that the silica-added hybrid gel showed the most significant improvement in terms of the storage modulus, an elastic component that characterizes the stiffness of the gel. The increase in stiffness of the polymeric hydrogels is considered to be favorable in applications for hard tissues, like bone and teeth.[33, 34] Here the issue is more detailed in relation with the cellular responses.

3.3. In vitro apatite forming ability and ionic releases of the hybrid hydrogels

The apatite forming behaviors of the hydrogels were monitored in SBF to presume the bone

bioactivity *in vitro*. The morphological changes of the hydrogels during the SBF-test were examined via SEM. While the collagen hydrogel showed no changes, Col-Sil hybrid gels exhibited development of fine crystallites throughout the gels (**Fig. 6a**). A closer examination of the produced crystals revealed the growth of flake-like highly-faceted nano-crystallites. The TEM image of the nano-crystallites (shown for Col-20S, representatively) reflected well the clustered nanoflakes of the crystals, and the selected-area election diffraction (SAED) signals revealed a spotted ring pattern, which was characteristic of apatite nano-crystals (**Fig. 6b**). The results indicated that Col-Sil hybrid hydrogels are expected to be very bone-bioactive *in vitro*, inducing apatite mineral growth throughout the hydrogel networks. The silica addition to the polymeric materials have been shown to improve the in vitro acellular mineralization elsewhere, including in silica-chitosan, silica-silk, and silica-collagen, prepared in the form of membranes and porous foams.[20, 35, 36] The highly negatively charged siloxane groups present in the silica phase played a key role in the deposition of calcium ions present in SBF, which in turn captured phosphate ions to accelerate the whole mineralization process.

The ionic releases from the hybrid hydrogels were monitored by ICP-AES for up to 3 weeks in PBS (**Fig. 7**). Since the hydrogels showed hydrolytic degradation in PBS, the silicon ions in the silica phase were considered to be released with time. The silicon release was observed for both the Col-10S and Col-20S, and it continued with time, showing higher amount from the Col-20S. The silicon release recorded for 21 days was ~40 ppm for Col-10S and ~70 ppm for Col-20S. The silicon ionic release from the hybrid hydrogels would positively affect the cell response during the culture experiments. Previous reports also highlighted the beneficial influence of the silicon ions leached from bioactive materials, such as glasses, coatings, and silicon-doped apatite.[37, 38] Bone-associated cells were stimulated to increase in proliferation and/or osteogenic differentiation when cultured with silicon-releasing matrices or dosed at proper concentrations.[37, 39] The silicon amounts recorded herein (tens of ppm) were also within the cell-stimulating ranges previously documented.[40]

Taking all the physico-chemical and mechanical properties as well as the degradation behaviors observed for the hydrogels, the silica-hybridized gels were considered to provide more favorable 3D environments for cells and the application of bone tissue engineering in terms of the structural and chemical stability, mechanical rigidity, and acellular bone bioactivity (silicon ionic release and mineralization acceleration).

3.4. Cell growth, associated hydrogel contraction, and osteogenesis

To assess whether the developed hydrogels can provide suitable 3D matrix conditions for cells to survive, grow, and adopt proper differentiation for bone tissues, we cultured MSCs derived from rat bone marrow within the hydrogels. First, the MSCs behaviors at the short time periods of up to 3 days were examined. The cells cultured within the gels were monitored by confocal microscopy (**Fig. 8a**). At day 1, some cells had cytoskeletal extensions while many cells were spherical with limited extensions. At day 3, the cell extensions were more pronounced and more cells were found. Next, the cell viability within the gels was monitored via MTS (**Fig. 8b**). The cell viability at day 1 was not significantly different for all groups, while slightly lower level at day 3 was noticed in Col-20S.

With prolonged culture of the cells, the gel matrices were shown to shrink since the collagen gel is well-known to undergo cell-mediated contraction.[41] The shrinkage of the hydrogels was thus examined. The initial cell densities varied (5×10^4, 1×10^5, and 2×10^5 cells/ml), and the cell-mediated gel contraction was measured at different culture periods. **Fig. 9** shows the cell-mediated contractions with varying cell densities in different hydrogel compositions. With 5×10^4 cells/ml (**Fig. 9a)**, the gel contractions were observed starting from 7 days and increased quite linearly with culture time for all groups. The contraction increase rate was in the following order: Col > Col-10S > Col-20S. Finally, the contractions were recorded at 21 days and were of approximately 50%, 35%, and 20%, for Col, Col-10S, and Col-20S, respectively. With 1×10^5 cells/ml (**Fig. 9b)**, the contractions in Col and Col-10S were abrupt at 7 days (down to 40–50%), which was then preserved for up to 21 days. On the other hand, the contraction behavior of Col-20S was different from that of the others, without showing an abrupt contraction at day 7 but rather a linear increase in contraction as was observed for the lower cell density. The contraction recorded at 21 days was approximately 70%, 65% and 50%, for Col, Col-10S and Col-20S, respectively. With 2×10^5 cells/ml (**Fig. 9c)**, all three groups presented similar behaviors, with a rapid contraction at day 7 and ongoing contraction for up to 21 days. The contractions recorded at 21 days were of approximately 90%, 78%, and 60%, for Col, Col-10S and Col-20S, respectively. Based on the gel contraction results, it was clear that the silica-hybridized hydrogels had less gel contraction for all cell densities and for all time points, and the higher silica content controlled these effects. Furthermore, the gel contractions were more pronounced when the cell density was higher and the culture period was longer, implying that this phenomenon was, as expected, closely related to the cell population.

As to the cell-induced gel contraction mechanisms, when the cells anchored and spread along the hydrogel networks, they exerted substantial contractile forces that shrink the gel networks. With an increase in the culture period, the cells multiplied to increase the contractile forces, and at the same time, the gel matrix was also degraded enzymatically as a result of the increased cell numbers, all of which consequently accelerate the shrinkage of the gel matrix. Therefore, the reduced contractions in the silica-hybridized gels were considered to primarily be a result of the increased resistance to the contractile forces induced by the cells since the hybrid gel was much stiffer. Together with a higher rigidity, the less degradable properties of the hybrid gels also contributed to the decreased gel contraction. This gel contraction behavior observed in the collagen-based hydrogels has become a significant obstacle to apply these gels in tissue engineering applications.[42] Therefore, such a decrease in gel contraction by silica hybridization is considered to be another beneficial point for the use of a hybrid gel matrix. Collectively, the hybrid gels provided favorable conditions for MSCs to survive, spread, and multiply, exerting substantial contractile forces on the gel networks to shrink consequently though with a lower level than that of collagen.

Next, the osteogenic differentiation of the cells cultured on collagen, Col-10S, and Col-20S hydrogels was investigated. First, the cell morphologies at 14-day culture were monitored by CLSM (**Fig. 10a**). The cells cultured on collagen were shown to develop well-spread and organized actin filaments. On the other hand, the silica-hybrid gels appeared to show more elongated cytoskeletal extensions with narrower yet specified directional growth. Next, the expression of osteogenic genes, including Runx2, OPN and BSP, was analyzed at 14 days via quantitative RT-PCR (**Fig. 10b**). All the genes were significantly stimulated when cultured in the hybrid gels, and the most remarkable change was observed in the BSP gene – with an increase as high as 7 times for Col-10S and 14 times for Col-20S. For the case of Runx2 and OPN, the increases were ~1.5–2 times. While Runx2 and OPN are relatively early osteogenic markers, BSP is engaged in much later stages for osteogenic differentiation.[43, 44] Therefore, a substantial stimulation of the BSP gene during a relatively long culture period of 14 days was thought to reflect high osteogenic potential of MSCs induced by the hybrid gel matrix. We next examined the BSP protein expression by cells cultured in collagen, Col-10S, and Col-20S gels for 14 days (**Fig. 10c**). The Western blot band intensity was much stronger in cells cultured particularly on Col-20S gels.

Collectively, the hybrid gel provided 3D environments for MSCs to adopt an osteogenic

lineage more effectively than the pure collagen gel, with stimulated expressions of osteogenic markers at the gene and protein levels. At this point, significantly different cell growth morphology, particularly at a prolonged culture for 14 days with more highly elongated and directional spreading in the hybrids, were thought to reflect the higher osteogenic differentiation status of the cells. In fact, previous studies on MSCs reported that those with better osteogenic differentiation had more elongated and higher cell aspect ratios, and this was observed when they were cultured on stiffer gel matrices or on nano-topological substrates.[45, 46]

There can be multiple reasons for osteogenic stimulation in the hybrid gels. First, the stiffer hybrid matrix can drive MSC differentiation into the osteogenic lineage. In fact, the storage modulus values of all compositions are well within the ranges similar to those of native non-calcified or collagenous bone matrices as well as those of demineralized bone matrices engineered, and this fact is considered to be favorable for cellular fate determination into hard tissue.[47-50] Thus, even pure collagen gel is considered to be favorable for driving cells down the osteogenic lineage. However, when cells proliferate actively and substantial collagen degradation is involved, the rigid matrix becomes softer, resulting in gel contraction driven by a cellular contractile force. Substantial gel contraction that occurred in pure collagen reflects well the change from a stiff to a soft gel matrix with increasing cell culture time. On the other hand, the hybrid gels have more rigid properties, and the cells can propagate and spread more effectively without causing substantial gel contraction. These different gel stiffnesses and cell-driven gel contraction behaviors between the hydrogel groups may result in dissimilar MSC differentiation and differential osteogenesis. At the same time, the release of silicon ions should also influence cellular fate. The silicon ions released (~tens of ppm) have been shown to positively influence the proliferation and differentiation of osteoblasts and stem cells. Together with the physical nature of the gels (stiffness and contraction), this chemical source (silicon ion) could alter the behavior of MSCs in a manner favorable for an osteogenic lineage.

4. Conclusions

Collagen-silica hydrogels were produced by a sol-gel process for hard tissue engineering. During the hydrolysis and condensation reactions, the silica components chemically linked with the collagen amino acid networks to form hybridized hydrogels. The hybrids improved the chemical stability of the

hydrogels, such as slowing down the enzymatic degradation. The hybrid gels exhibited improved mechanical properties, including a higher resistance to static stress and a storage modulus in dynamic conditions. The silica-addition also enhanced the in vitro apatite forming ability in SBF of the hydrogels. The MSCs cultured within the hydrogels were shown to actively spread and proliferate, which resulted in substantial hydrogel contractions. The silica-containing compositions reduced the gel contraction significantly, and the osteogenic differentiation of the MSCs was greatly enhanced by the hybrid hydrogels in terms of the bone-related gene and protein expressions. The developed silica-collagen hybrid hydrogels, according to the results of the physico-chemical and mechanical as well as the degradation test in parallel with MSC growth and osteogenic differentiation behaviors, indicate this material may be a potential matrix for bone tissue engineering.

Acknowledgements

This work was supported by the Priority Research Centers Program through the National Research Foundation of Korea (NRF) funded by the Ministry of Education, Science, and Technology (grant No. 2009-0093829).

References

1. El-Sherbiny IM, Yacoub MH. Hydrogel scaffolds for tissue engineering: Progress and challenges. *Glob. Cardiol. Sci. Pract.* 2013;2013:316-342
2. Ferreira AM, Gentile P, Chiono V, Ciardelli G. Collagen for bone tissue regeneration. *Acta Biomater.* 2012;8:3191-3200
3. Geckil H, Xu F, Zhang X, Moon S, Demirci U. Engineering hydrogels as extracellular matrix mimics. *Nanomed. Nanotechnol. Biol. Med.* 2010;5:469-484
4. Jia X, Kiick KL. Hybrid multicomponent hydrogels for tissue engineering. *Macromol. Biosci.* 2009;9:140-156
5. Drury JL, Mooney DJ. Hydrogels for tissue engineering: Scaffold design variables and applications. *Biomaterials*. 2003;24:4337-4351
6. Hunt NC, Grover LM. Cell encapsulation using biopolymer gels for regenerative medicine. *Biotechnol. Lett.* 2010;32:733-742
7. Nicodemus GD, Bryant SJ. Cell encapsulation in biodegradable hydrogels for tissue engineering applications. *Tissue Eng. Pt. B-Rev.* 2008;14:149-165
8. Zhu J, Marchant RE. Design properties of hydrogel tissue-engineering scaffolds. *Expert Rev. Med. Devices*. 2011;8:607-626
9. Leslie-Barbick JE, Shen C, Chen C, West JL. Micron-scale spatially patterned, covalently immobilized vascular endothelial growth factor on hydrogels accelerates endothelial tubulogenesis and increases cellular angiogenic responses. *Tissue Eng. Pt. A*. 2010;17:221-229
10. Yun Y-R, Won JE, Jeon E, Lee S, Kang W, Jo H, Jang J-H, Shin US, Kim H-W. Fibroblast growth factors: Biology, function, and application for tissue regeneration. *J. Tissue Eng.* 2010;1:218142
11. Perez RA, Won J-E, Knowles JC, Kim H-W. Naturally and synthetic smart composite biomaterials for tissue regeneration. *Adv. Drug Del. Rev.* 2013;65:471-496
12. Bae W-J, Min K-S, Kim J-J, Kim J-J, Kim H-W, Kim E-C. Odontogenic responses of human dental pulp cells to collagen/nanobioactive glass nanocomposites. *Dent. Mater.* 2012;28:1271-1279
13. Glowacki J, Mizuno S. Collagen scaffolds for tissue engineering. *Biopolymers*. 2008;89:338-344
14. Lee CH, Singla A, Lee Y. Biomedical applications of collagen. *Int. J. Pharm.* 2001;221:1-22
15. Thoma DS, Jung RE, Schneider D, Cochran DL, Ender A, Jones AA, Görlach C, Uebersax L, Graf-Hausner U, Hämmerle CH. Soft tissue volume augmentation by the use of collagen-based matrices: A volumetric analysis. *J. Clin. Periodontol.* 2010;37:659-666
16. El-Fiqi A, Lee JH, Lee E-J, Kim H-W. Collagen hydrogels incorporated with surface-aminated mesoporous nanobioactive glass: Improvement of physicochemical stability and mechanical properties is effective for hard tissue engineering. *Acta Biomater.* 2013;9:9508-9521
17. Lickorish D, Ramshaw JA, Werkmeister JA, Glattauer V, Howlett CR. Collagen-hydroxyapatite composite prepared by biomimetic process. *J. Biomed. Mater. Res. A*. 2004;68:19-27
18. Pighinelli L, Kucharska M. Chitosan-hydroxyapatite composites. *Carbohydr. Polym.* 2013;93:256-262
19. Heinemann S, Heinemann C, Bernhardt R, Reinstorf A, Nies B, Meyer M, Worch H, Hanke T. Bioactive silica-collagen composite xerogels modified by calcium phosphate phases with adjustable mechanical properties for bone replacement. *Acta Biomater.* 2009;5:1979-1990

20. Arcos D, Vallet-Regí M. Sol-gel silica-based biomaterials and bone tissue regeneration. *Acta Biomater.* 2010;6:2874-2888
21. Yang P, Gai S, Lin J. Functionalized mesoporous silica materials for controlled drug delivery. *Chem. Soc. Rev.* 2012;41:3679-3698
22. Desimone MF, Hélary C, Quignard S, Rietveld IB, Bataille I, Copello GJ, Mosser G, Giraud-Guille M-M, Livage J, Meddahi-Pellé A. In vitro studies and preliminary in vivo evaluation of silicified concentrated collagen hydrogels. *ACS Appl. Mater. Sci. Interface*. 2011;3:3831-3838
23. Desimone MF, Hélary C, Rietveld IB, Bataille I, Mosser G, Giraud-Guille M-M, Livage J, Coradin T. Silica-collagen bionanocomposites as three-dimensional scaffolds for fibroblast immobilization. *Acta Biomater.* 2010;6:3998-4004
24. Fagundes L, Sousa T, Sousa A, Silva V, Sousa E. Sba-15-collagen hybrid material for drug delivery applications. *J. Non-Cryst. Solids*. 2006;352:3496-3501
25. Heinemann S, Coradin T, Desimone MF. Bio-inspired silica-collagen materials: Applications and perspectives in the medical field. *Biomater. Sci.* 2013;1:688-702
26. Heinemann S, Coradin T, Worch H, Wiesmann H, Hanke T. Possibilities and limitations of preparing silica/collagen/hydroxyapatite composite xerogels as load-bearing biomaterials. *Compos. Sci. Technol.* 2011;71:1873-1880
27. Yun YR, Lee S, Jeon E, Kang W, Kim KH, Kim HW, Jang JH. Fibroblast growth factor 2-functionalized collagen matrices for skeletal muscle tissue engineering. *Biotechnol Lett*. 2012;34:771-778
28. Oh S-A, Lee H-Y, Lee JH, Kim T-H, Jang J-H, Kim H-W, Wall I. Collagen three-dimensional hydrogel matrix carrying basic fibroblast growth factor for the cultivation of mesenchymal stem cells and osteogenic differentiation. *Tissue Eng. Pt. A*. 2012;18:1087-1100
29. Seo S-J, Kim J-J, Kim J-H, Lee J-Y, Shin US, Lee E-J, Kim H-W. Enhanced mechanical properties and bone bioactivity of chitosan/silica membrane by functionalized-carbon nanotube incorporation. *Compos. Sci. Technol.* 2014;96:31-37
30. Baccile N, Babonneau F, Thomas B, Coradin T. Introducing ecodesign in silica sol-gel materials. *J. Mater. Chem.* 2009;19:8537-8559
31. Gelinsky M, Welzel P, Simon P, Bernhardt A, König U. Porous three-dimensional scaffolds made of mineralised collagen: Preparation and properties of a biomimetic nanocomposite material for tissue engineering of bone. *Chem. Eng. J.* 2008;137:84-96
32. Asran AS, Henning S, Michler GH. Polyvinyl alcohol-collagen-hydroxyapatite biocomposite nanofibrous scaffold: Mimicking the key features of natural bone at the nanoscale level. *Polymer*. 2010;51:868-876
33. Singh RK, Patel KD, Kim J-J, Kim T-H, Kim J-H, Shin US, Lee E-J, Knowles JC, Kim H-W. Multifunctional hybrid nanocarrier: Magnetic cnts ensheathed with mesoporous silica for drug delivery and imaging system. *ACS Appl. Mater. Sci. Interface*. 2014;6:2201-2208
34. Kim J-J, Singh RK, Seo S-J, Kim T-H, Kim J-H, Lee E-J, Kim H-W. Magnetic scaffolds of polycaprolactone with functionalized magnetite nanoparticles: Physicochemical, mechanical, and biological properties effective for bone regeneration. *RSC Adv.* 2014;4:17325-17336
35. Ruiz-Hitzky E, Darder M, Aranda P, Ariga K. Advances in biomimetic and nanostructured biohybrid materials. *Adv. Mater.* 2010;22:323-336
36. Mieszawska AJ, Nadkarni LD, Perry CC, Kaplan DL. Nanoscale control of silica particle formation via silk− silica fusion proteins for bone regeneration. *Chem. Mater.* 2010;22:5780-5785
37. Hoppe A, Güldal NS, Boccaccini AR. A review of the biological response to ionic dissolution products from bioactive glasses and glass-ceramics. *Biomaterials*. 2011;32:2757-2774

38. Xu S, Lin K, Wang Z, Chang J, Wang L, Lu J, Ning C. Reconstruction of calvarial defect of rabbits using porous calcium silicate bioactive ceramics. *Biomaterials*. 2008;29:2588-2596
39. Gorustovich AA, Roether JA, Boccaccini AR. Effect of bioactive glasses on angiogenesis: A review of in vitro and in vivo evidences. *Tissue Eng. Pt. B-Rev.* 2009;16:199-207
40. Oh S-A, Kim S-H, Won J-E, Kim J-J, Shin US, Kim H-W. Effects on growth and osteogenic differentiation of mesenchymal stem cells by the zinc-added sol-gel bioactive glass granules. *J. Tissue Eng.* 2010;1:475260
41. Sung KE, Su G, Pehlke C, Trier SM, Eliceiri KW, Keely PJ, Friedl A, Beebe DJ. Control of 3-dimensional collagen matrix polymerization for reproducible human mammary fibroblast cell culture in microfluidic devices. *Biomaterials*. 2009;30:4833-4841
42. Brigham MD, Bick A, Lo E, Bendali A, Burdick JA, Khademhosseini A. Mechanically robust and bioadhesive collagen and photocrosslinkable hyaluronic acid semi-interpenetrating networks. *Tissue Eng. Pt. A*. 2008;15:1645-1653
43. Yu H-S, Won J-E, Jin G-Z, Kim H-W. Construction of mesenchymal stem cell-containing collagen gel with a macrochanneled polycaprolactone scaffold and the flow perfusion culturing for bone tissue engineering. *Biores Open Access*. 2012;1:124-136
44. Duvall CL, Taylor WR, Weiss D, Wojtowicz AM, Guldberg RE. Impaired angiogenesis, early callus formation, and late stage remodeling in fracture healing of osteopontin-deficient mice. *J. Bone Miner. Res.* 2007;22:286-297
45. Oh S, Brammer KS, Li YJ, Teng D, Engler AJ, Chien S, Jin S. Stem cell fate dictated solely by altered nanotube dimension. *Proc. Natl. Acad. Sci. USA*. 2009;106:2130-2135
46. Dalby MJ, Gadegaard N, Tare R, Andar A, Riehle MO, Herzyk P, Wilkinson CD, Oreffo RO. The control of human mesenchymal cell differentiation using nanoscale symmetry and disorder. *Nat. Mater.* 2007;6:997-1003
47. Engler AJ, Sen S, Sweeney HL, Discher DE. Matrix elasticity directs stem cell lineage specification. *Cell* 2006;126:677-89.
48. Catanese J 3rd, Iverson EP, Ng RK, Keaveny TM. Heterogeneity of the mechanical properties of demineralized bone. *J Biomech* 1999;32:1365-9.
49. Summitt MC, Reisinger KD. Characterization of the mechanical properties of demineralized bone. *J Biomed Mater Res A*. 2003;67(3):742-50
50. Hamed E, Novitskaya E, Li J, Chen PY, Jasiuk I, McKittrick J. Elastic moduli of untreated, demineralized and deproteinized cortical bone: validation of a theoretical model of bone as an interpenetrating composite material. *Acta Biomater*. 2012;8(3):1080-92.

Graphical Abstract:

Hybrid hydrogels comprising of collagen-silica demonstrated excellent chemical stability and bone-bioactivity, and the stem cell cultivation and osteogenic responses, ultimately favorable for bone tissue engineering.

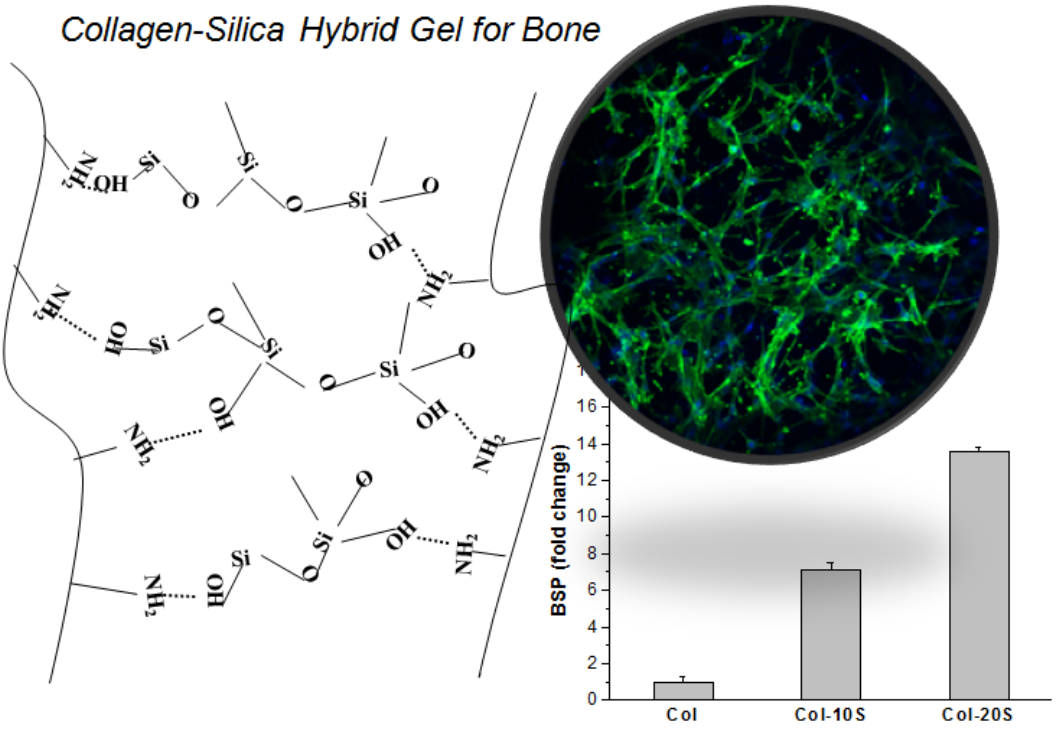

568 **Fig. 1.** Schematic drawing of the Col/Sil hybrid hydrogel system, illustrating the formation of

569 hybridized networks between the two components.

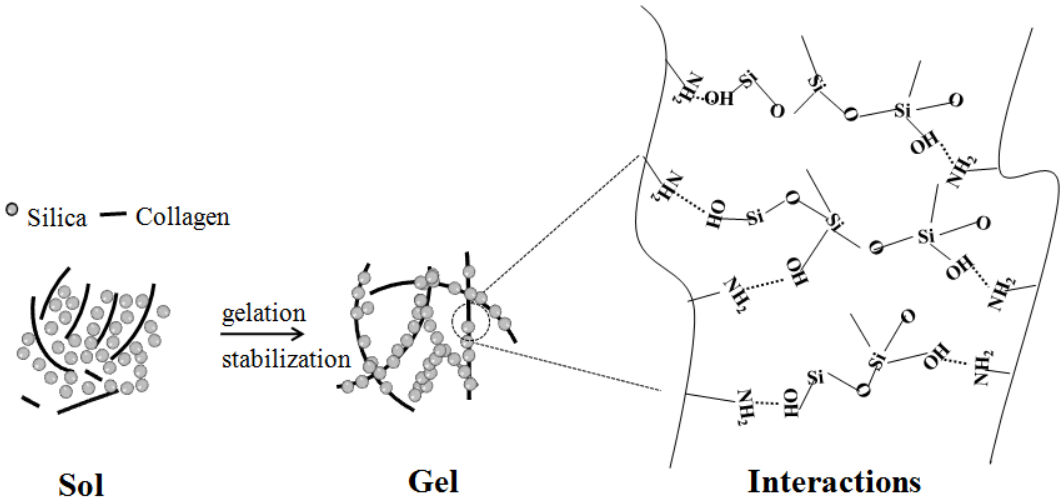

570

571

Fig. 2. (a,b) FT-IR spectrum observed at wide and narrow ranges, and (c) collagen denaturation temperature recorded from DSC curves of the hydrogels with different compositions. Closer examination of the FT-IR in a narrow range revealed a blue shift of the collagen amide band with silica hybridization. Collagen denaturation temperature increased with silica hybridization.

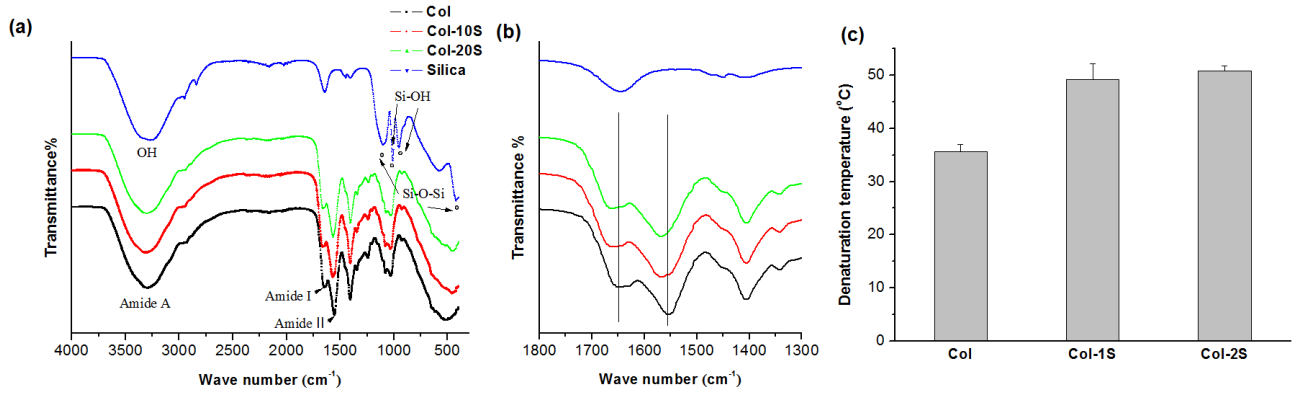

Fig. 3. Enzymatic degradation of hydrogels measured for up to 120 min, using collagenase type I (54 U/ml) in Tris-HCL buffer. Statistical significance was noticed for the hybrid gels vs. Col gel at each time point (*p < 0.05, n = 3).

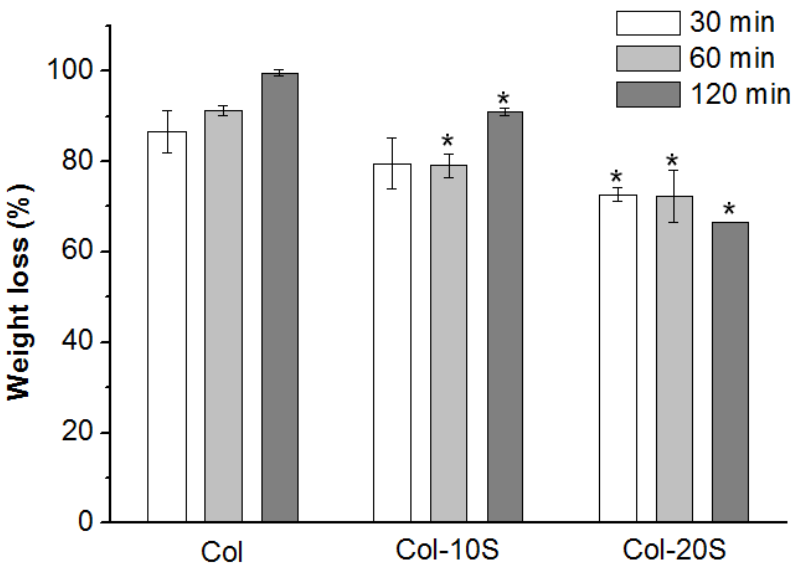

Fig. 4. Static mechanical properties of collagen, Col-10S, and Col-20S hydrogels. (a) Static strain change with constant stress applied for 450 s. Initial slope values (strain rate) were also fitted. (b) Stress recorded at 450 s.

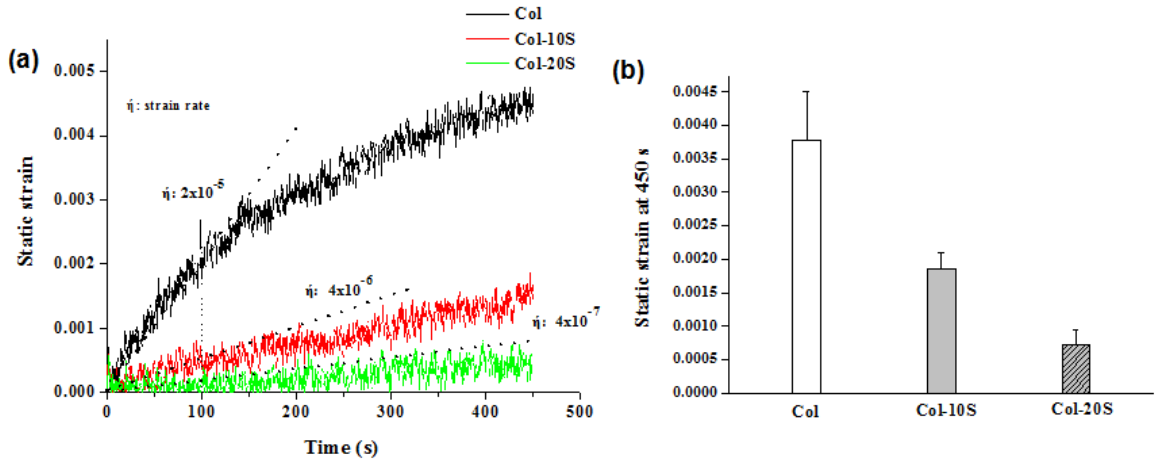

Fig. 5. Dynamic mechanical analysis of collagen, Col-10S, and Col-20S hydrogels. (a) E' and E" variations with frequency change, (b) average E' and E" values obtained, and (c) tan delta (E"/E', loss factor).

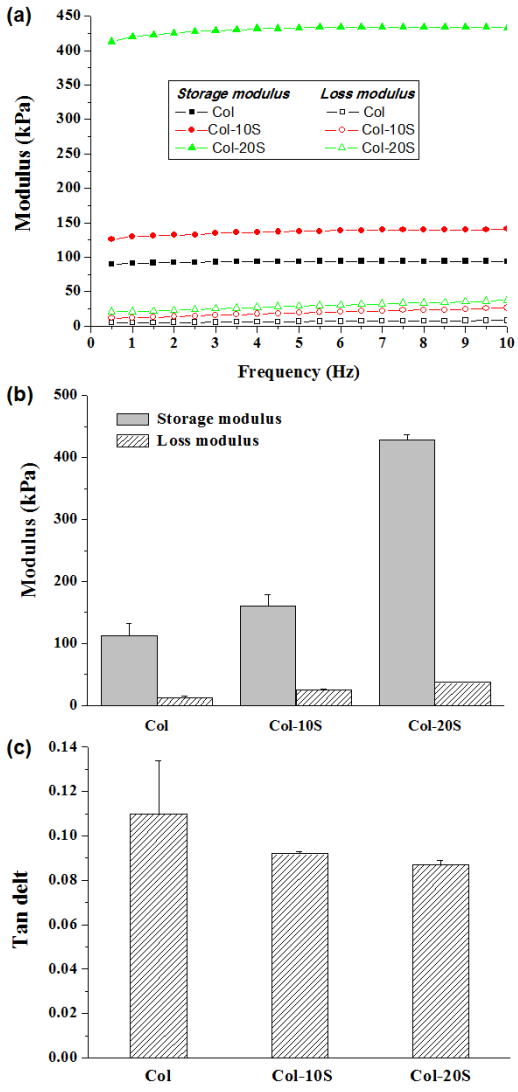

Fig. 6. In vitro apatite-forming ability assessed by an SBF-immersion test. (a) The SEM morphology of collagen, Col-10S, and Col-20S hydrogels at 7 days, and (b) TEM image and SAED pattern at 7 days (Col-20S shown for representative sample), revealing hydroxyapatite crystalline structure.

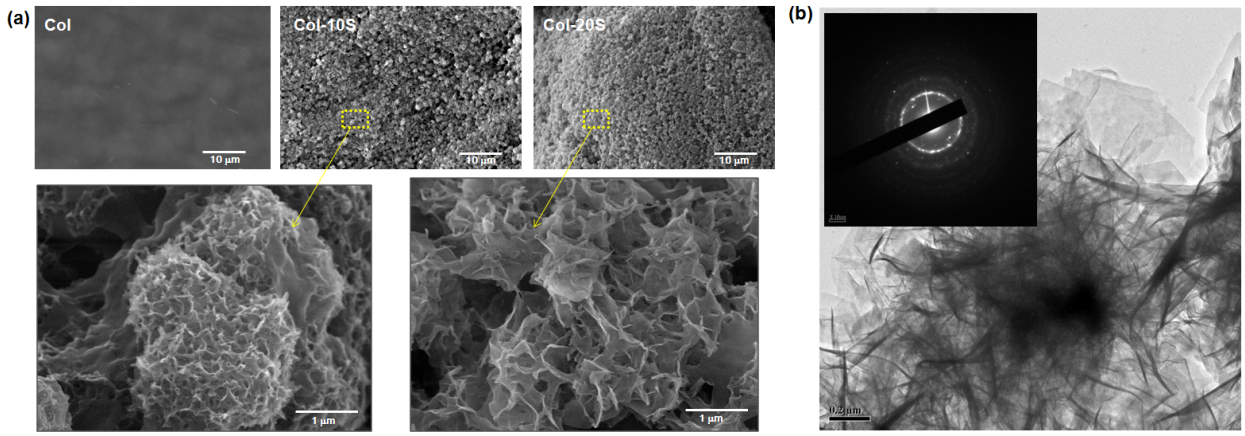

Fig. 7. Silicon ion release (in ppm) from the hydrogels, monitored via ICP-AES for up to 3 weeks in PBS.

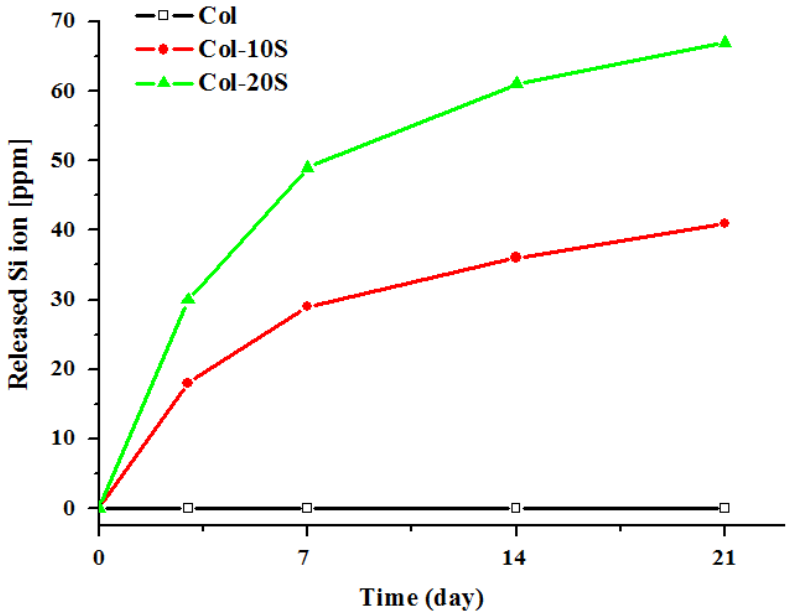

608 **Fig. 8.** (a) Cell growth morphology at day 1 and 3 observed by CLSM. Cell nuclei stained in blue
609 (DAPI) and cytoskeletons in green (Alex fluor 488 phalloidin). (b) Cell viability determined by MTS.
610

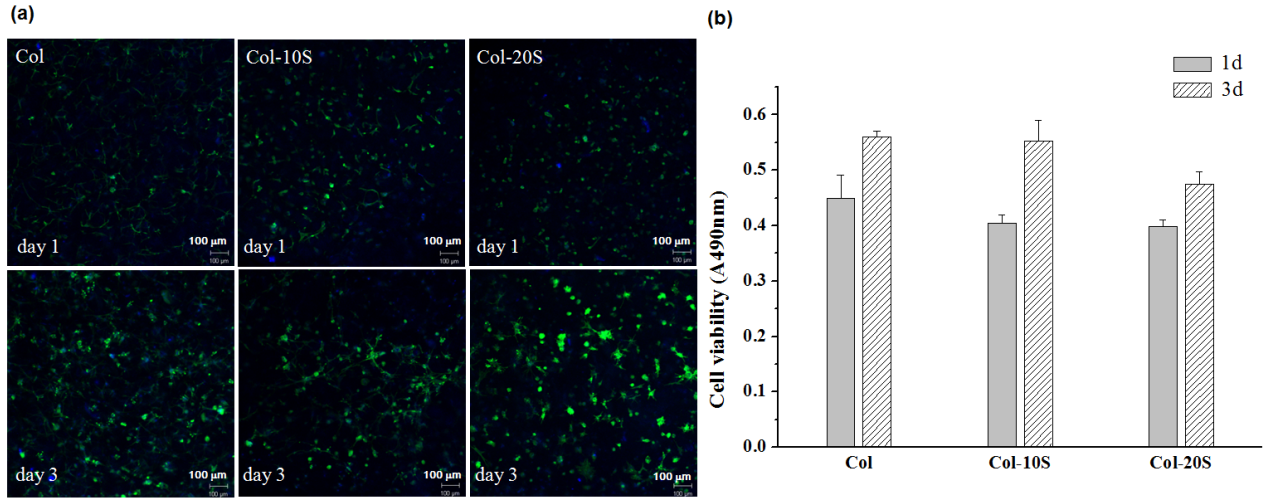

611
612

Fig. 9. Cell-mediated hydrogel contraction with culture for up to 21 days. Different cell densities were used; (a) 5 x 10^4, 1 x 10^5 and (c) 1 x 10^5 cells/ml.

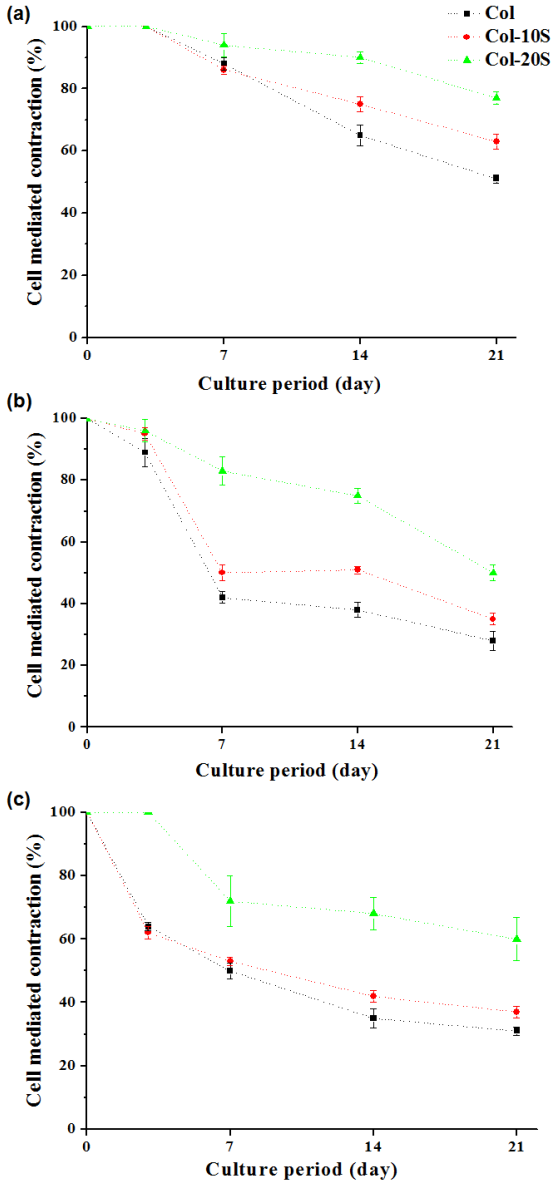

Fig. 10. (a) Cell growth morphology within the hydrogels at day 14, observed by CLSM. (b) Expression of osteogenic markers, OPN and BSP, by quantitative RT-PCR, and (c) BSP protein analyzed by Western blot at day 14.